Redox Biology 59 (2023) 102560

Contents lists available at ScienceDirect

Redox Biology

journal homepage: www.elsevier.com/locate/redox

Identification of galectin-1 and other cellular targets of alpha, beta-unsaturated carbonyl compounds, including dimethylfumarate, by use of click-chemistry probes

Max B. Sauerland [a], Christina Helm [a], Lasse G. Lorentzen [a], Asmita Manandhar [b], Trond Ulven [b], Luke F. Gamon [a], Michael J. Davies [a,*]

[a] Department of Biomedical Sciences, Panum Institute, University of Copenhagen, Copenhagen, 2200, Denmark
[b] Department of Drug Design and Pharmacology, Jagtvej 162, University of Copenhagen, Copenhagen, 2100, Denmark

ARTICLE INFO

Keywords:
Dimethylfumarate
Unsaturated carbonyls
Michael adduct
Click chemistry
Galectin
Electrophile

ABSTRACT

α,β-Unsaturated carbonyls are a common motif in environmental toxins (e.g. acrolein) as well as therapeutic drugs, including dimethylfumarate (DMFU) and monomethylfumarate (MMFU), which are used to treat multiple sclerosis and psoriasis. These compounds form adducts with protein Cys residues as well as other nucleophiles. The specific targets ('adductome') that give rise to their therapeutic or toxic activities are poorly understood. This is due, at least in part, to the absence of antigens or chromophores/fluorophores in these compounds. We have recently reported click-chemistry probes of DMFU and MMFU (Redox Biol., 2022, 52, 102299) that allow adducted proteins to be visualized and enriched for further characterization. In the current study, we hypothesized that adducted proteins could be 'clicked' to agarose beads and thereby isolated for LC-MS analysis of DMFU/MMFU targets in primary human coronary artery smooth muscle cells. We show that the probes react with thiols with similar rate constants to the parent drugs, and give rise to comparable patterns of gene induction, confirming similar biological actions. LC-MS proteomic analysis identified ~2970 cellular targets of DMFU, ~1440 for MMFU, and ~140 for the control (succinate-probe) treated samples. The most extensively modified proteins were galectin-1, annexin-A2, voltage dependent anion channel-2 and vimentin. Other previously postulated DMFU targets, including glyceraldehyde-3-phosphate dehydrogenase (GAPDH), cofilin, p65 (RELA) and Keap1 were also identified as adducted species, though at lower levels with the exception of GAPDH. These data demonstrate the utility of the click-chemistry approach to the identification of cellular protein targets of both exogenous and endogenous compounds.

1. Introduction

The alpha,beta-unsaturated carbonyl compound dimethylfumarate and its metabolite monomethylfumarate (DMFU and MMFU respectively, Fig. 1) show potent anti-inflammatory and antioxidant activity, and are used clinically as drugs to treat psoriasis (under the trade names 'Fumaderm' and 'Skilarence') and multiple sclerosis (MS, under the name 'Tecfidera' and 'Bafiertam') [1,2]. It is probable that MMFU is the active species in each case, while DMFU acts as a pro-drug and is converted to MMFU by esterases or chemical hydrolysis before entering the systemic circulation. Experimental data derived from studies on animal models have suggested that DMFU also has potential benefits in other diseases associated with chronic inflammation including atherosclerosis [3], Alzheimer's [4] and Parkinson's diseases [5], and other conditions [6]. These data have resulted in significant efforts to repurpose DMFU and MMFU for alternative treatments [6]. A derivative of DMFU, diroximel fumarate (2-(2,5-dioxopyrrolidin-1-yl)ethyl methyl fumarate, trade name 'Vumerity', a species with one of the methyl groups substituted with a 2-(2,5-dioxopyrrolidin-1-yl)ethyl function) was approved for clinical use to treat MS by the FDA 2019, and by the EU in 2021 [7,8]. Diroximel fumarate can also act as a pro-drug for MMFU, with hydrolysis occurring in the intestine. This compound appears to give rise to fewer side-effects when compared to DMFU [9], where at least some of the DMFU side-effects can be ascribed to methanol generated by ester hydrolysis.

Multiple sclerosis is an autoimmune disease involving the central nervous system (CNS). Relapsing-remitting periods of symptom-

* Corresponding author.
E-mail address: davies@sund.ku.dk (M.J. Davies).

https://doi.org/10.1016/j.redox.2022.102560
Received 16 November 2022; Received in revised form 26 November 2022; Accepted 26 November 2022
Available online 1 December 2022

Abbreviations used

ACN	acetonitrile
CAA	chloroacetamide
DMF	dimethylformamide
DMFU	dimethylfumarate
DMFU-P	DMFU-probe, dimethylfumarate with a methyl group substituted with a butylalkyne function
DMSO	dimethylsulfoxide
EAE	experimental autoimmune encephalomyelitis
GAPDH	glyceraldehyde-3-phosphate dehydrogenase
HCASMC	human coronary artery smooth muscle cells
iBAQ	intensity-based absolute quantification
LDH	lactate dehydrogenase
MMFU	monomethylfumarate
MMFU-P	MMFU-probe, monomethylfumarate with the methyl group substituted with a butylalkyne function
NAC	*N*-acetylcysteine
TCEP	tris(2-carboxyethyl) phosphine
TFA	trifluoroacetic acid
THPTA	tris(3-hydroxypropyltriazolylmethyl)amine

manifestation characterize the initial phases of this disease, which later transforms into a more neurodegenerative type [10]. MS is diagnosed via lesion development in the CNS induced by autoreactive immune cells, including TH1 and TH17 cells. The current treatment strategy relies on immune suppression, which is able to reduce symptoms and the numbers of CNS-homing immune cells. However, this treatment strategy does not stop disease progression, and only modulates the rate of development [10].

Psoriasis is another immunological disorder in which T-cell activation results in an auto-inflammation of the skin and other organs. Treatment of psoriasis with IL-17A inhibitors has shown beneficial effects, consistent with an important role of this pro-inflammatory cytokine, which acts as a regulator of NF-kappaB and mitogen-activated protein (MAP) kinases, in the disease [11]. Interestingly, anti-IL-17A treatment has also shown therapeutic benefit in the treatment of atherosclerosis, which can be present as a comorbidity with psoriasis [12].

As DMFU and MMFU are alpha,beta-unsaturated carbonyl compounds, they can act as soft electrophiles which react with the thiol (-SH) or the more reactive thiolate ($-S^-$) functions of cysteine (Cys) residues in target proteins [13]. These Michael addition reactions (Fig. 1) result in the formation of long-lived (succinylated) adduct species that can alter the structure of proteins or impair enzymatic activity. Whilst Cys residues present at physiological pH values in their thiolate form (i.e. those with a low pK_a value) show enhanced reactivity when compared to non-ionized Cys, the association between these parameters has been shown to be weak [13], and multiple other factors including steric and electronic factors also determine the rate constants for adduct formation. Thus, these soft electrophiles typically show a modest specificity for biological targets, and are often avoided in drug discovery programs, unless they contain additional features that impart a greater degree of targeting [14].

DMFU and MMFU have a long clinical history in the treatment of psoriasis, starting from 1959 and widespread marketing from 1994, however their critical biological targets have not been definitively established. Although there is evidence available for reactions for DMFU and MMFU with hundreds of proteins, which (and how many) of these contribute to its pharmacological actions is unknown, and the majority of these are likely to be bystander reactions of no biological impact, or worse, responsible for adverse side-effects [15,16]. The latter include (usually modest) gastrointestinal effects (nausea, diarrhoea, abdominal pain), flushing and lymphopenia, but can include more serious effects. DMFU is also a powerful contact allergen [17]. Uncovering the key targets responsible for both the positive and negative effects of DMFU/MMFU may therefore aid the development of new drugs (e.g. analogues such as itaconate [18,19]) and accelerate drug repurposing.

Proposed targets of DMFU/MMFU include GAPDH [20], IRAK4 [21], Cofilin [22], and Keap1 [23]. Each of these proteins contains one or more Cys residues, whose modification is reported to inhibit protein function, and have anti-inflammatory effects. Keap1 is the most widely discussed key DMFU target [23,24]. The modification of this protein leads to decreased level of tagging (ubiqitinylation) of its binding partner NRF2 for proteasomal degradation. This decreased rate of NRF2 removal allows newly synthesized NRF2 (which is a potent master regulator of genes involved in metabolism, inflammation, autophagy,

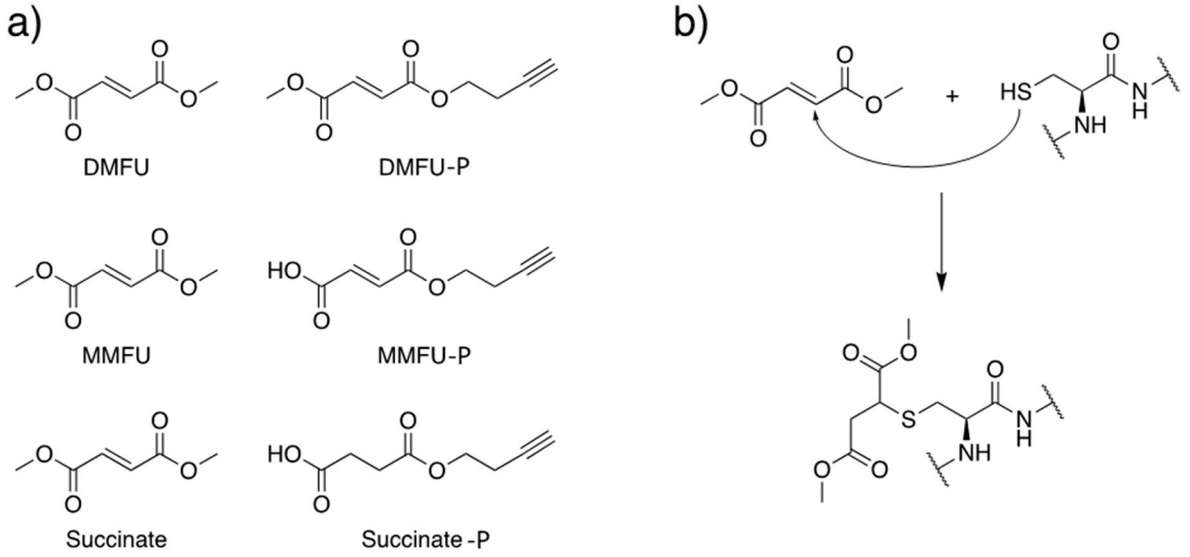

Fig. 1. (a) Chemical structures of dimethylfumarate (DMFU), monomethylfumarate (MMFU), succinate, and their respective alkyne-tagged probes (DMFU-P/MMFU-P/succinate-P). The succinate probe lacks the double bond and is therefore unreactive and used as a negative control. (b) Michael adduction reaction between DMFU and cysteine. The electrophilic beta carbon from DMFU is attacked by a (nucleophilic) electron pair of the thiol or thiolate anion of cysteine to yield a new covalent thioether bond.

protein turnover, immune responses, and mitochondrial physiology) to enter the nucleus, and bind to antioxidant response elements (AREs). DMFU has been shown to be of benefit in a myelin oligodendrocyte glycoprotein-induced multiple sclerosis mouse model, but fails to do so in NRF2$^{-/-}$ mice [25]. Whilst adduction to Cys151 (and other Cys residues) in Keap1 is widely reported to be responsible for these effects, evidence has also been provided for DMFU binding (in a non-covalent manner, and at nanomolar levels) to other sites on Keap1, including the NRF2 binding site and the blade II site of the beta-propeller domain [26]. Other studies have however suggested that modulation of Keap1-NRF2 interactions is not essential to DMFUs anti-inflammatory actions. Thus, DMFU protected wild type and NRF2$^{-/-}$ mice equally well from inflammatory experimental autoimmune encephalomyelitis [27]. Furthermore, multiple proteomic studies of the DMFU-sensitive proteome have failed to identify Keap1 as a target ([15,28,29], reviewed [30]), though this may be a sensitivity issue. Other targets of DMFU/MMFU have also been proposed (reviewed [30]).

In the study reported here, we aimed to utilize recently developed alkyne tagged (probe) versions of DMFU and MMFU (DMFU-P and MMFU-P respectively, Fig. 1), which can be used for click chemistry to examine the cellular targets of DMFU/MMFU [31]. We have shown previously that the presence of the alkyne substituent allows visualization [31] of the proteins that are targets of adduction via copper-catalyzed click chemistry addition of a fluorophore. In the current study, we use a related approach to enrich samples with DMFU/MMFU targets, by binding the adducted proteins to azide-linked agarose beads, with subsequent LC-MS analysis of the DMFU-/MMFU--sensitive proteome of the cells. This has allowed elucidation of the "modificome" generated by these drugs, and the identification of both proposed and novel targets of these species.

2. Material and methods

2.1. Chemicals

Trypsin-EDTA, *N*-acetylcysteine (NAC), trifluoroacetic acid (TFA), Triton X-100, sodium pyruvate, sodium deoxycholate, tris(2-carboxyethyl)phosphine (TCEP), 2-chloroacetamide, bovine serum albumin, sodium dodecyl sulfate, tris(3-hydroxypropyltriazolylmethyl) amine (THPTA), monomethylfumarate (MMFU), succinate, dimethylfumarate (DMFU), copper(II) sulfate pentahydrate, Tween-20, sodium ascorbate, NADH and ethanol were obtained from Sigma-Aldrich/Merck (Søborg, Denmark). Chambered cover glass slides, 20x PBS, paraformaldehyde, Vectrashield mounting media, Tris Base, acetonitrile (ACN), HEPES buffer, urea, isopropanol, formic acid (FA) and Sera-Mag carboxylate-modified magnetic particles (SP3 beads; cat. no. 44152105050250 and 24152105050250, mixed 1:1) were from VWR (Søborg, Denmark). DAPI, NuPage LDS sample buffer, NU-Page 3–8% Bis-Tris gels, NU-Page MES running buffer, NuPage reducing agent, Lipofectamine™ RNAiMAX transfection reagent, Silencer™ Select predesigned siRNA for galectin-1, recombinant human galectin-1 and Alexa-488 azide were from Thermo (Roskilde, Denmark). RNeasy Kit and DNAse were from Quiagen (Copenhagen, Denmark). Sequencing grade trypsin was from Promega (Finnboda, Sweden). Reverse transcription kit and SensSensiFAST® SYBR Hi-ROX Kit were from Nordic Biosite (Stockholm, Sweden). Precision Plus Protein™ Kaleidoscope™ Standards were from Biorad (Copenhagen, Denmark), and Azure 700 from Azure (Dublin, US). Growth media for primary human coronary artery smooth muscle cells (HCASMC) was purchased from tebu-bio (Roskilde, Denmark). The alkyne-tagged derivatives of DMFU, MMFU and succinate (used as a negative control as it lacks the reactive double bond), were synthesized as described previously [31].

2.2. Determination of rate constants for reaction of MMFU/MMFU-probe and DMFU-probe with N-acetylcysteine (NAC)

A method developed previously, was employed to examine the kinetics of reaction of alkyne-tagged DMFU and MMFU with NAC [13]. In brief, reaction mixtures were prepared by mixing the soft electrophiles (250 μM) with NAC (500 μM) in 1x PBS, pH 7.4. Aliquots were removed, at the indicated time points, and the reactions stopped by the addition of TFA to 0.6% (v/v). The samples were subsequently analyzed by HPLC against standards as described previously, with loss of the electrophile monitored over time. Plotting $Ln\frac{Electrophile_0 * NAC_t}{NAC_0 * Electrophile_t} * \frac{1}{Electrophile_0 - NAC_0}$, where the subscripts $_0$ and $_t$ indicates the concentrations at time zero and time t, respectively, against the reaction time provides a linear graph with the slope of the plot giving the second order reaction rate constants (k_2). The linear regression line of the plots was calculated using the Graphpad Prism linear regression function, with significant differences in the gradients (k_2) between the probe and parent compounds assessed using Student's t-test.

2.3. Cell culture

Human coronary artery smooth muscle cells (HCASMC, donor #1522; tebu-bio) were cultured until 80% confluent in smooth muscle cell growth medium at 37 °C and 5% CO_2. The cells were then detached using trypsin-EDTA for 5 min, and the cell numbers adjusted to 5×10^4 cells mL^{-1} in growth media and seeded according to the assay. Galectin-1 knockdown was performed with galectin-1-siRNA and lipofectamine; the reagents were mixed according to the manufacturer's instructions, and added to the plate before the cells were seeded. The lactate dehydrogenase (LDH) assay was carried out in a 24-well plate format, with 0.5 mL cell suspension. Immunocytochemistry was carried using eight-well chambered cover glass with 0.2 mL of cell suspension. The qPCR experiments employed 12-well plates with 1 mL of cell suspension. HCASMC proteomic experiments, including those using galectin-1 knockdown, were carried out using 6-well plates with 2 mL of cell suspension. The azide-agarose click-chemistry experiments used T25 flasks with 10 mL of cell suspension. All plates containing the cells were cultured for 24 h before treatment with parent drugs, drug probes, or control solutions.

2.4. Lactate dehydrogenase assay

HCASMC (2.5×10^4 cells per well, in a 24 well plate) were treated with 0–200 μM of DMFU, MMFU or the corresponding probes in growth media for 24 h. The supernatants were then collected, and the cells were lysed in H_2O with scraping of the cells. Lysis was confirmed by microscopic examination. LDH activity was assessed in both the supernatants and the cell lysates by adding 0.23 mM NADH and 2.5 mM sodium pyruvate in PBS; 200 μL of this solution was then added to 10 μL of lysate or supernatant and the rate of change in absorbance at 340 nm was used to determine the LDH activity. The relative viability was calculated using the standard method of activity in supernatant over total activity (supernatant plus lysate) x 100. Statistical analyses were carried out using Graphpad Prism 9.3, by 2-way ANOVA with Šídák's multiple comparison test.

2.5. Gene expression

HCASMC (5×10^4 cells per well, in a 12 well plate) were treated with DMFU/MMFU, or the respective probes, for 24 h at 50 μM. RNA extraction was performed using a RNeasy kit according to the manufacturer's instructions, including an on-filter DNA digestion. The RNA concentration was measured using a Clariostar plus system according to the manufacturer's instructions. cDNA synthesis was conducted with 250 ng RNA in 38.5 μL water. Reverse transcriptase (1.5 μL) and 10 μL

TransAmp buffer were then added before placement in a thermocycler (5 min at 25 °C, 30 min at 42 °C, 5 min at 85 °C, hold at 4 °C). The cDNA was then diluted to 2.5 ng μL^{-1}. For qPCR a SensiFAST® SYBR Hi-ROX Kit was used following the manufacturer's instructions with the primer pairs used at 10 μM. Primer sequences are given in Supplementary Table 1 qPCR was performed using a Quant Studio 5 system and analyzed with the provided software. Statistical analyses were carried out using GraphPad Prism 9.3 by one-way ANOVA following ΔΔCt analysis.

2.6. Click chemistry and subsequent analysis of adducts by fluorescence and immunoblotting with co-staining

HCASMC (1×10^4 cells per well, in a 8-well chambered glass slide with covers) were treated with 100 μM DMFU-probe for 15 min at 37 °C. The cells were then fixed using paraformaldehyde (4%, 15 min), and permeabilized with Triton X-100 (0.1%, 10 min). The treated cells (and controls) where then incubated with a click chemistry master mix consisting of $CuSO_4$ (2 mM), Alexa-488 azide (3 μM), and ascorbic acid (110 mM) in 1x PBS for 15 min. DAPI was used for nuclear staining. Co-staining was carried out by blocking the cells with BSA in TBST (3%, 30 min) before incubating the cells with the primary anti-body (1:100 dilution for Galectin1-ab108389, 1h, in 3% BSA in TBST). The cells were then washed with PBST and incubated with an appropriate Alexa-594 conjugated secondary antibody for 1 h in TBST containing 3% BSA (w/v). The cells were subsequently washed and covered with Vectra shield mounting medium. Cell images were captured using a Zeiss LSM 780 confocal microscope using the following conditions: DAPI, λ_{ex} 405 nm, λ_{em} 454 nm; DMFU probe, λ_{ex} 488 nm, λ_{em} 525 nm; Galectin1, λ_{ex} 595 nm, λ_{em} 668 nm.

2.7. Immunoblotting

HCASMC (1×10^5 cells per well, in 6-well plates) were treated with 100 μM of DMFU-, MMFU- or succinate-probe (4 h for the DMFU probe, 24 h for the MMFU and succinate probes, due to their slower reaction kinetics). The cells were then lysed in 1 mL lysis buffer (1% SDS in 50 mM Tris, pH 7.8). The lysates (50 μL) were then subjected to click chemistry by adding sequentially 2 μL $CuSO_4$ (50 mM stock), 8 μL Alexa-488-azide (100 mM stock), 10 μL THPTA (25 mM stock), 5 μL DMSO, 3 μL sodium ascorbate (600 mM stock), and 10 μL aminoguanidine hydrochloride (150 mM stock); the samples were then incubated for 2 h at 21 °C in the dark. The samples were then subjected to a clean-up protocol by precipitation of the proteins onto mixed SP3 beads (4 μL) by addition of 70% ACN in H_2O and incubation for 20 min. The beads where then separated from the reaction mixture using a magnetic rack and washed once with 70% ethanol in H_2O and twice with 100% ACN. Proteins where then eluted from the beads using 20 μL of 2x NuPage loading buffer and 1x NuPage reducing agent, with incubation at 60 °C for 15 min. 15 μL of each sample was then loaded on to a 3–8 Bis-Tris gel with appropriate fluorescent marker proteins and run for 35 min at 170 V. The separated proteins were then transferred to a membrane using an iBlot 2 Dry Blotting system, following the manufacturer's instructions. The membrane was blocked with BSA (3% in TBST, 1 h) and incubated with the primary antibody (1:1000 dilution for Galectin1-ab108389, overnight, in 3% BSA in TBST). The membrane was then washed and incubated with a secondary antibody (Azure-700, 1:10,000, in 3% BSA in TBST) for 1 h. The membrane was then washed again, imaged with a Sapphire Biomolecular Imager (Azure Bioscience), and analyzed with Azure spot software.

2.8. Sample preparation for liquid chromatography-mass spectrometry (LC-MS)

Proteins (5 μg, galectin-1; 10 μg cell lysates) were precipitated onto magnetic SP3 beads (4 μL, 1:1 mixture) in 70% ACN. The beads were then washed once with 70% ethanol in H_2O, and twice with 100% ACN, before being reduced using TECP (10 mM) and alkylated using CAA (40 mM) in 0.1 M TEBA by incubation for 20 min at 60 °C. The beads are then subject to on-bead digestion to peptides, using a ratio of 20:1 protein:trypsin (37 °C, overnight). The digest was then cleaned up via solid-phase extraction utilizing C-18 material as the solid phase, after activation of the solid phase with ethanol, and equilibration with 0.1% TFA. The digest was acidified to pH 2, using TFA, then loaded onto the solid phase, washed once with 0.1% TFA in H_2O, then eluted with 0.1% TFA in 80% ACN in H_2O. The digest was dried down under vacuum, reconstituted in 5% FA in H_2O, and subjected to LC-MS using a timsTOF Pro mass spectrometer (Bruker, Bremen) after separation using a Dionex Ultimate RSLCnano system (Thermo Scientific) with an Aurora series reversed-phase C18 column (25 cm × 75 μm i.d., 1.6 μm C18, IonOpticks) at 60 °C. A 100 min gradient of 2–25% B, where mobile phase A was 0.1% formic acid in water, and B was 0.1% formic acid in acetonitrile, was used to separate peptides. Data were acquired either in data-independent-acquisition (DIA) mode (for the galectin-1 knockdown proteomics) or in a data-dependent-acquisition (DDA) mode (azide-bead experiments and galectin-1 modifications).

2.9. Alkyne probe-based proteomics

The click-chemistry protocol employed has been described previously [32]. HCASMC were treated with 100 μM DMFU-, MMFU- or succinate-probe as described above, with the treated cells then scraped into PBS, spun down (220 g, 2 min) and the pellet lysed in 100 μL heated lysis buffer (4% SDS, 80 °C). DNA was removed by hydrolysis using TFA (11 μL, 10%, 30 min), with the samples then neutralized by adding 360 μL H_2O and 25 μL Tris base (2 M). Samples of lysate (500 μL) were then subjected to click-chemistry, by adding sequentially $CuSO_4$ (to 1 mM), THTPA (to 2.5 mM), azide-derivatized agarose beads (60 μL), DMSO (to 5%), sodium ascorbate (to 15 mM) and aminoguanidine hydrochloride (to 1 mM), in a total volume of 750 μL, and incubated overnight at 21 °C. The beads were then washed 4 times with a mixture of 2.5% SDS and 2.5% SDC heated to ~80 °C, 4 times with a mixture of 100 mM HEPES and 8 M urea, twice with 50% isopropanol in H_2O, twice with 50% ACN in H_2O, and once with digestion buffer consisting of 50 mM HEPES, 1.6 M urea and 5% ACN in H_2O. The beads were then resuspended in 40 μL digestion buffer and subjected to reduction with tris(2-carboxyethyl) phosphine (TECP, 10 mM) and alkylation with 2-chloroacetamide (CAA, 40 mM) at 60 °C for 20 min. The proteins were then digested using 6 μL of trypsin (0.1 μg μL^{-1}) overnight at 37 °C. Clean-up of the samples and LC-MS analysis was carried out as described above (Section 2.8.) starting at the solid phase extraction stage. The raw data were searched against the human UniProtKB/Swiss-Prot database (UP 000005640, reviewed sequences, downloaded 2022-10-20) using MSFragger (v3.5) implemented in fragpipe (v18.0). Intensity-based absolute quantification (IBAQ) values were calculated according to the method described in Ref. [33]. Briefly, for each identified protein, all matching peptide intensities were summed and then divided by the number of theoretically observable peptides in the database with lengths between 7 and 35 amino acids (identical search constraints to those used by MSFragger). Data from three independent treatments of the cells were analyzed and are reported.

2.10. Proteome analysis of galectin-1 knocked-down HCASMC

Untreated or galectin-1 knocked down cells (Section 2.3., 1×10^5 cells per well, in 6-well plates) were incubated with DMFU and MMFU (25 μM, 24 h) and lysed in 200 μL lysis buffer (5% SDS in 50 mM Tris, pH 7.8, 21 °C). The DNA was hydrolysed by adding TFA (1% final concentration, 30 min), then neutralized with 720 μL H_2O and 50 μL Tris base (2 M). The samples were subsequently prepared and analyzed as described in Section 2.8, using a data-independent acquisition, parallel accumulation-serial fragmentation (DIA-PASEF) protocol. Data analyses

were carried out using DIA-NN (v1.8.1) in library-free mode. Further data processing, analysis, and visualization were then performed using the programming language R. Normalized precursor-level intensities were extracted from the DIA-NN report, and the MsqRobSum workflow was used for the analysis of differential protein expression. Proteins were considered as differentially expressed if the Benjamin–Hochberg adjusted p-value was <0.01.

2.11. Analysis of recombinant galectin-1 treated with DMFU or MMFU

Recombinant human galectin-1 (5 μg) was treated with 250 μM DMFU or MMFU (1 h, 21 °C) in 10 μL PBS. The modified galectin-1 was then reduced and alkylated as described in Section 2.8. Samples were then subjected to clean up using SP3 beads (see Section 2.8) and digested overnight with 0.4 μg trypsin at 37 °C. The samples were then subjected to solid phase extraction (see Section 2.8). LC-MS analysis was done on an Impact II QTOF mass spectrometer (Bruker Daltonics) in the positive ion mode with a CaptiveSpray ion source on-line connected to a Dionex Ultimate 3000 chromatography system (Thermo Fisher Scientific). Peptides were separated on a 150 × 0.5 mm, 5 μm particle size C18(2) 100 Å Luna column (Phenomenex) at 20 °C with a solvent gradient over 38 min, using water with 0.1% formic acid (Solvent A) and acetonitrile with 0.1% formic acid (Solvent B) at a flow rate of 20 μL min^{-1} (0–27 min, 5–40% B; 27–29 min, 40–95% B; 29–35 min, 95% B; 35–36 min 95-5% B; 36–38 min 5% B). The mass spectrometer was operated in data-dependent mode (DDA) for the top 3 precursor ions with a cycle time of 3 s at 4–16 Hz.

2.11. Statistical analyses and errors

Statistical analyses were carried out using features within GraphPad Prism version 9, as described in the individual sections, and reflect data from three independent experiments. Kinetic data were assessed using linear correlation analysis. Other data were assessed using 2-way ANOVA with subsequent multiple comparison tests.

3. Results

3.1. DMFU/MMFU and their respective alkyne-tagged probes show similar rate constants for reaction with N-acetylcysteine (NAC)

We have previously reported rate constants, k_2, for the reaction of DMFU with a range of thiols, including those with different pK_a values, and examined the correlation between the k_2 values and thiol pK_a: these values show only a weak association, indicating that other factor also influence the rate constants [13]. Data for MMFU were not reported, nor for the alkyne-substituted species. As a consequence, it was of interest and potential importance, to determine if DMFU and MMFU react with thiols with similar k_2 values, and whether the alkyne function of the probe species results in major differences relative to the parent. Rate constants were therefore determined for reaction with NAC using the previously validated kinetic method [13]. The concentrations of residual MMFU/DMFU-P/MMFU-P remaining after reaction with NAC at particular time points were determined by UPLC and plotted against reaction time (Fig. 2). These data yielded linear plots (Fig. 2a–c) consistent with the kinetic model employed (single direct biomolecular reactions). The resulting gradients yielded the second order rate constants, k_2 (Fig. 2d). Comparison of the data for DMFU-P with DMFU (reported in Ref. [13]), indicates that the alkyne function results in a small increase in k_2 (~1.8-fold). As expected, the value of k_2 for MMFU was significantly lower than for DMFU (~75 fold), with this consistent with the lower reported reactivity of MMFU compared to DMFU [34]. The value for MMFU-P was slightly higher than for MMFU (~1.4-fold), as seen with the DMFU/DMFU-P pairing. These data indicate that the alkyne probes react in a similar manner to the parent compounds, and with comparable rate constants, indicating that the reactivity of the probes closely mimics that of the parent drugs.

3.2. DMFU/MMFU and their respective alkyne-tagged probes show similar biological effects on HCASMC

Related experiments to those described above, were carried out to

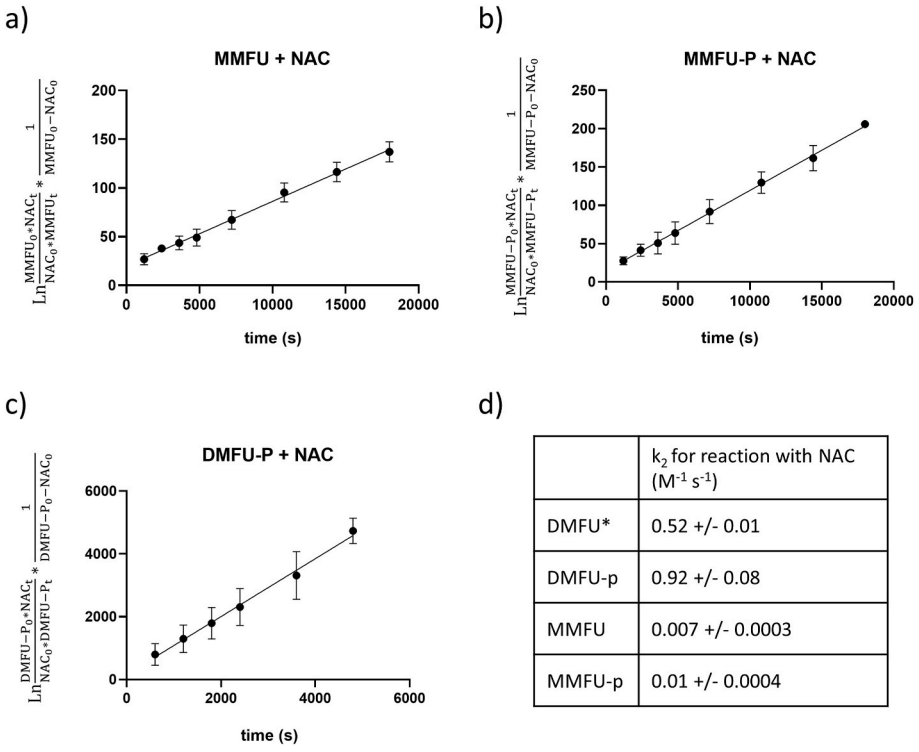

d)

	k_2 for reaction with NAC (M^{-1} s^{-1})
DMFU*	0.52 +/- 0.01
DMFU-p	0.92 +/- 0.08
MMFU	0.007 +/- 0.0003
MMFU-p	0.01 +/- 0.0004

Fig. 2. The alkyne probes of DMFU (DMFU-P) and MMFU (MMFU-P) react with N-acetylcysteine (NAC) with rate constants that are similar to those of the parent compounds. (A–C) Kinetic analysis plots for the reactions of DMFU-P, MMFU-P and parent MMFU (all 250 μM) with 500 μM NAC. The change in concentration of the parent or probe compounds was measured over time by UPLC and the corresponding data analyzed as indicated in the Materials and methods. The kinetic plots yield straight lines consistent with the proposed bimolecular (2nd order) mechanism, with the gradients of the plots yielding the second order reaction rate constants, k_2 (summarized in panel d). * Data from Ref. [13] obtained by the same method under identical conditions.

examine whether the alkyne-tagged species have similar biological properties and activity to the parents. HCASMC were treated with increasing concentrations (0–200 μM) of DMFU/MMFU, or their corresponding probes for 24 h, before assessment of the extent of cell viability (as determined by the release of intracellular LDH into the extracellular medium). After incubation for 24 h, both DMFU and DMFU-P showed a similar decrease in cell viability, with the loss in cell viability increasing in a concentration-dependent manner (Fig. 3a). No statistically significant differences were detected between DMFU and DMFU-P. In addition, no significant differences were detected between MMFU and MMFU-P (Fig. 3b), though the extent of cytotoxicity detected with MMFU was significantly less than with DMFU, consistent with its lower reactivity (see above).

As both DMFU and MMFU can drive the transcription of anti-oxidative and protective genes, such as heme oxygenase 1 (HOX-1) and glutathione reductase (GR), the induction of these genes was examined using qPCR. Treatment of HCASMC with 50 μM concentrations of the parent compounds or probes for 24 h, resulted in increased transcription when compared to untreated cells (Fig. 3c and d). The extent of gene induction by DMFU versus DMFU-P, and MMFU versus MMFU-P, were not statistically different (Fig. 3c and d). These data are consistent with a previous report indicating that the protein targets of DMFU/MMFU and the alkyne probes are similar [31].

3.3. Click chemistry adduction of alkyne-tagged proteins allows LC-MS identification of the molecular targets of DMFU and MMFU in HCASMC

The alkyne motif in the DMFU and MMFU probes can be utilized in reactions with azide compounds to give new 1,2,3-triazole rings via click-chemistry [35,36]. We postulated that this would allow enrichment of DMFU and MMFU adducted proteins, via the alkyne probes, when used with azide-derivatized agarose beads.

HCASMC were treated with 25 μM DMFU-P, MMFU-P or the corresponding succinate alkyne probe (as a control for non-specific binding) for 24 h. The HCASMC were then lysed and the probe-modified proteins clicked to azide agarose beads. The beads were then washed extensively, to remove non-covalently bound proteins, and the remaining proteins subjected to on-bead trypsin digestion and LC-MS analysis of the release peptides (Fig. 4).

Analysis of the resulting peptides from the DMFU-P treated samples indicated the presence of ~2970 adduct-containing proteins (3241 ± 39, n = 3 independent replicates, Supplementary Fig. 1), that were common to all samples, indicating that DMFU-P reacts with a large number of proteins. Analogous experiments with MMFU-P detected ~1440 adducted proteins (1842 ± 243) common to all samples. In contrast, only ~140 (230 ± 38) proteins were identified in experiments using the succinate probe, consistent with a low background of non-specific binding to the agarose beads (Fig. 5a, Supplementary Table 2). The top 20 'hits' detected with DMFU-P and MMFU-P are reported in Fig. 5d and e respectively; a full list is provided in

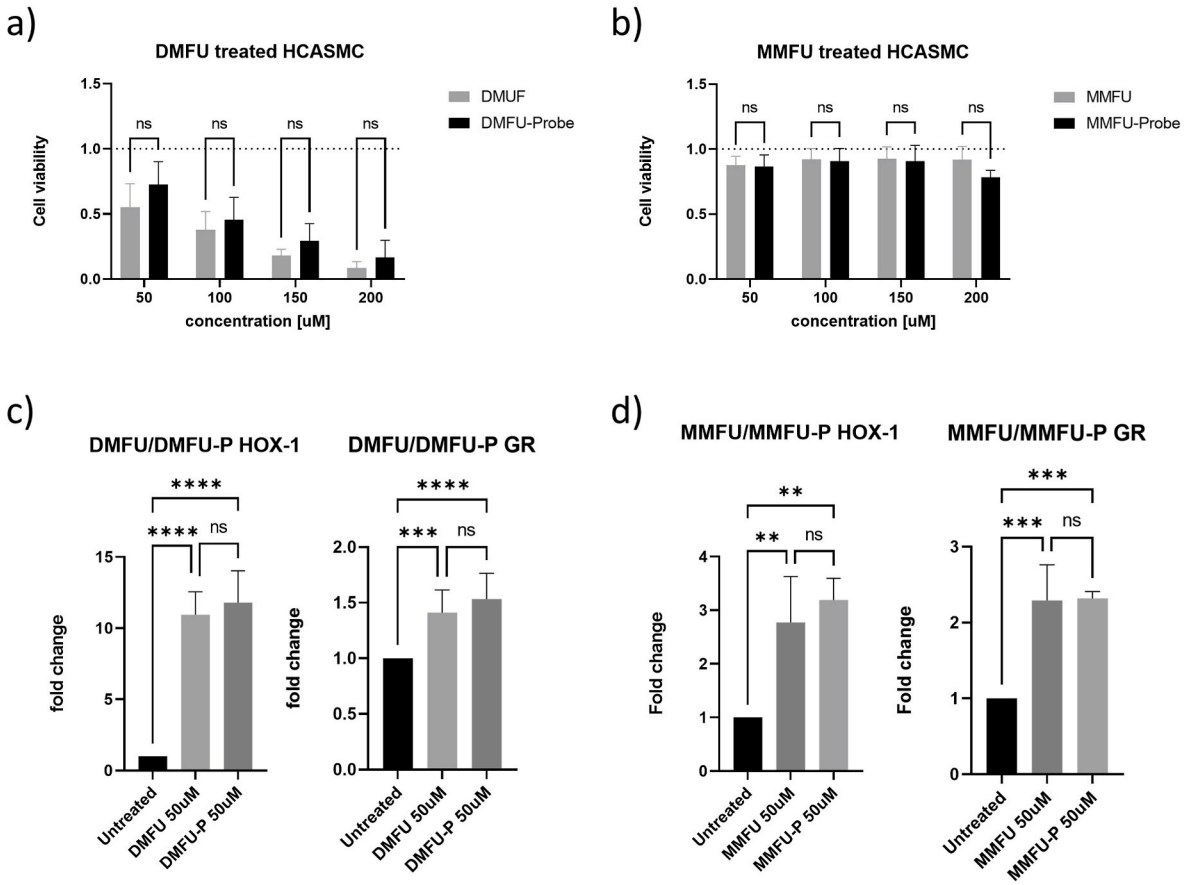

Fig. 3. The alkyne-tagged compounds show similar biological activities as the parent compounds. (a, b) HCASMC were treated for 24 h with the indicated concentrations of DMFU, MMFU or the corresponding probes. DMFU and the DMFU-P displayed comparable cytotoxicity under these conditions as determined by LDH release from the treated cells (see Materials and methods), expressed relative to untreated cells. MMFU and MMFU-P did not show significant cytotoxicity under the conditions investigated. (c, d) qPCR data showing the induction of heme oxygenase-1 (HOX-1) and glutathione reductase (GR) mRNA in HCASMC treated with DMFU or MMFU and their respective probes (each 50 μM, 24 h). Data are presented as mean ± SD from three independent experiments. Statistical analysis revealed that both the parent compounds and probes activate gene expression to the same extent.

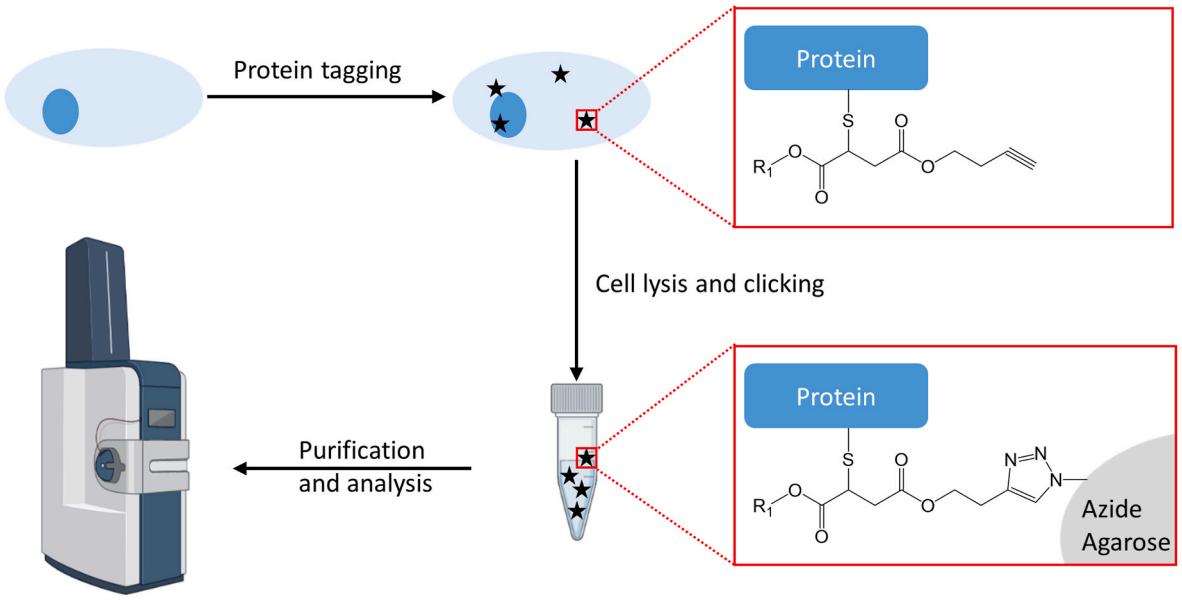

Fig. 4. Outline of workflow used to identify alkyne-tagged proteins adducted by DMFU-P and MMFU-P. HCASMC were treated with DMFU-P, MMFU-P or succinate-P (each 25 μM, 24 h) and then subsequently processed as described in the Materials and methods, before LC-MS analysis. Figure generated using Biorender.

Supplementary Table 2). These proteins were confirmed to contain one or more Cys residues (as determined by the mature protein sequences listed in the UniProt database), consistent with reaction of DMFU and MMFU at such residues. A possible caveat on this dataset is that some proteins (e.g. polyubiquitin-B) may not contain direct adducts, but be covalently bound to other proteins, and be recovered by the enrichment process without being direct targets of the probe. As MMFU is the major metabolite of DMFU, and the likely active species *in vivo* (cf. the use of MMFU, and diroximelfumarate to treat MS [6,8]), subsequent work focused on proteins that were detected as targets of both DMFU-P and MMFU-P. In order to assess whether the top 'hits' are determined by protein abundance (rather than reactivity with the probe), intensity-based absolute quantification (IBAQ) analyses were also carried out to determine the total proteome of the cells. In these analyses, the abundance of a protein is determined by dividing the total precursor ion intensities by the number of theoretically observable peptides of the protein [33]. It should be noted that this is not an ideal quantitative parameter, as the values are also affected by digestion and ionization efficiency, common problems in most MS quantification methods. The corresponding top 20 'hits' for protein abundance, as determined by this parameter for HCASMC, are presented in Fig. 5c. Comparison of these plots indicates that there are clear differences between the top 'hits' in Fig. 5d and e, versus Fig. 5c, suggesting that abundance is not the main driver of the top targets detected with the DMFU-P and MMFU-P probes (Supplementary Fig. 2). It should be noted that the intensity data presented in Fig. 5c cannot be directly compared to those in Fig. 5d and e due to the differences in experimental protocols.

The identifications presented in Fig. 5d and e and Supplementary Table 2, include a number of previously reported DMFU targets, including GAPDH [20], Cofilin [22], and Keap1 [23]. However, with the exceptions of GAPDH (which is present in the MMFU-P data set, Fig. 5e, but not that for DMFU) and Cofilin (CFL1, present in all three lists) these proteins do not feature in the list of most abundant adduct targets. The top identifications were galectin-1 (LGALS1), annexin-A2 (ANXA2), vimentin (VIM) and actin beta (ACTB) for DMFU-P, and galectin-1, VDAC2, GAPDH, and protein transport protein Sec61 subunit beta (SEC61B) for MMFU-P. As galectin-1 was the top target for both probes and was markedly more intense than the next highest candidate in both cases, this protein was chosen for further study.

3.4. Confirmation that galectin-1 is a target for DMFU and MMFU in HCASMC via orthogonal approaches

Confirmation that galectin-1 is a target for DMFU-P and MMFU-P was obtained using both immunocytochemistry and immunoblotting. In the former case, HCASMC were treated with DMFU-P (100 μM, 15 min, see Materials and methods), and the resulting cell samples were then subjected to click chemistry adduction with the azide-tagged fluorophore Alexa-488. The cell preparations were also probed using an antibody against galectin-1, and subsequently an Alexa-594 conjugated secondary antibody, and co-stained with DAPI to identify cell nuclei (Fig. 6a). The cells were then examined by fluorescence microscopy. This showed that the targets of DMFU-P are distributed widely throughout the cells, and on multiple species, as expected from the LC-MS data. Galectin-1 was also observed to be distributed in a diffuse manner throughout the cell cytosol, with merging of the images showing co-localization (Fig. 6a).

Immunoblotting was carried out on lysates from DMFU-P, MMFU-P or succinate-P treated cells (100 μM probe, 4 h). Cell proteins were separated by SDS-PAGE, then transferred to membranes and either imaged directly for fluorescence (Alexa-488 tagged species) or probed for galectin-1 using the anti-galectin antibody as described above. The Alexa-488 label fluorescence (Fig. 6b) revealed numerous adducted protein bands from the cells treated with DMFU-P or MMFU-P, but not the succinate probe, consistent with the non-reactivity of the succinate species, and the LC-MS data reported above. The membrane probed using the galectin-1 antibody showed a single band at ~15 kD (Fig. 6b, red fluorescence) as expected from the protein sequence. This band co-localized with a band detected by direct (Alexa-488, green) fluorescence supporting the conclusion that DMFU-P and MMFU-P react with galectin-1 in HCASMC.

3.5. LC-MS examination of recombinant human galectin-1 modification by DMFU and MMFU

The reactivity of galectin-1 with DMFU and MMFU was confirmed by analysis of recombinant human galectin-1 (5 μg) treated with DMFU or MMFU (250 μM, 1 h). LC-MS analysis using peptide mass mapping, showed a sequence coverage of 96% (Fig. 7a). The samples treated with either DMFU or MMFU yielded peptides consistent with modification at

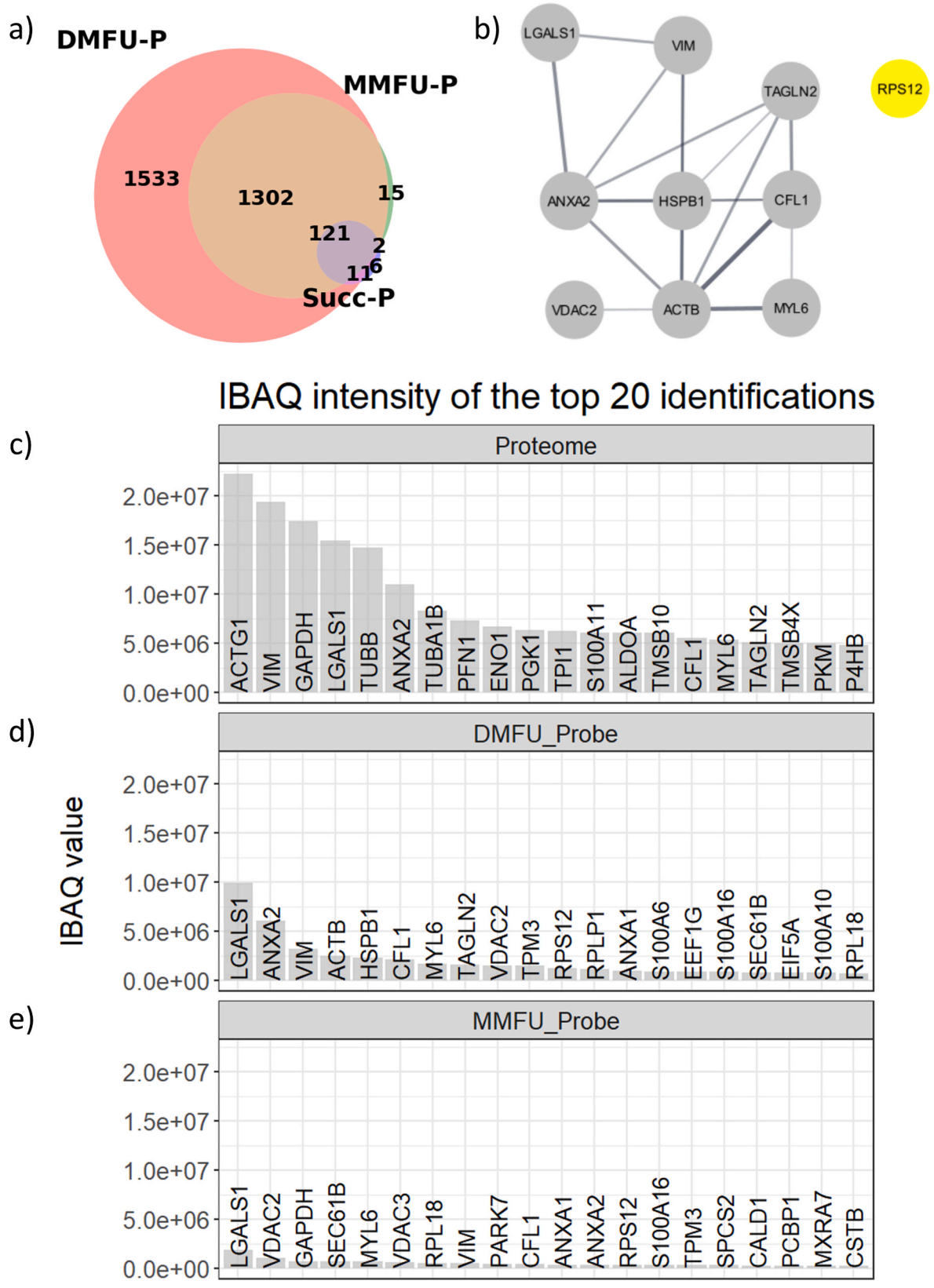

Fig. 5. (a) Venn diagram indicating the overlap in adducted proteins detected from treatment of HCASMC treated with DMFU-P, MMFU-P or succinate-P (each 25 μM, 24 h) and subsequent pulldown by click chemistry tagging to azide-derivatized beads and LC-MS analysis. DMFU-P was observed to modify ~2970 proteins, MMFU-P modifies ~1440 proteins and the succinate-P ~140 proteins (background hits). 1302 non-background proteins were detected as modified by both DMFU-P and MMFU-P. (b) String database analysis of the relationship between the proteins identified as the top 10 DMFU-probe hits, indicating that many of the top hits have close interactions, with the exception of RPS12 (colored yellow). (c) The 20 most abundant proteins detected by LC-MS analysis of HCASMC lysates (see Materials and methods) in the absence of alkyne tag treatment, pulldown or enrichment. (d, e) The 20 most adducted proteins from the DMFU-P or the MMFU-P pulldown experiments as calculated from iBAQ values.

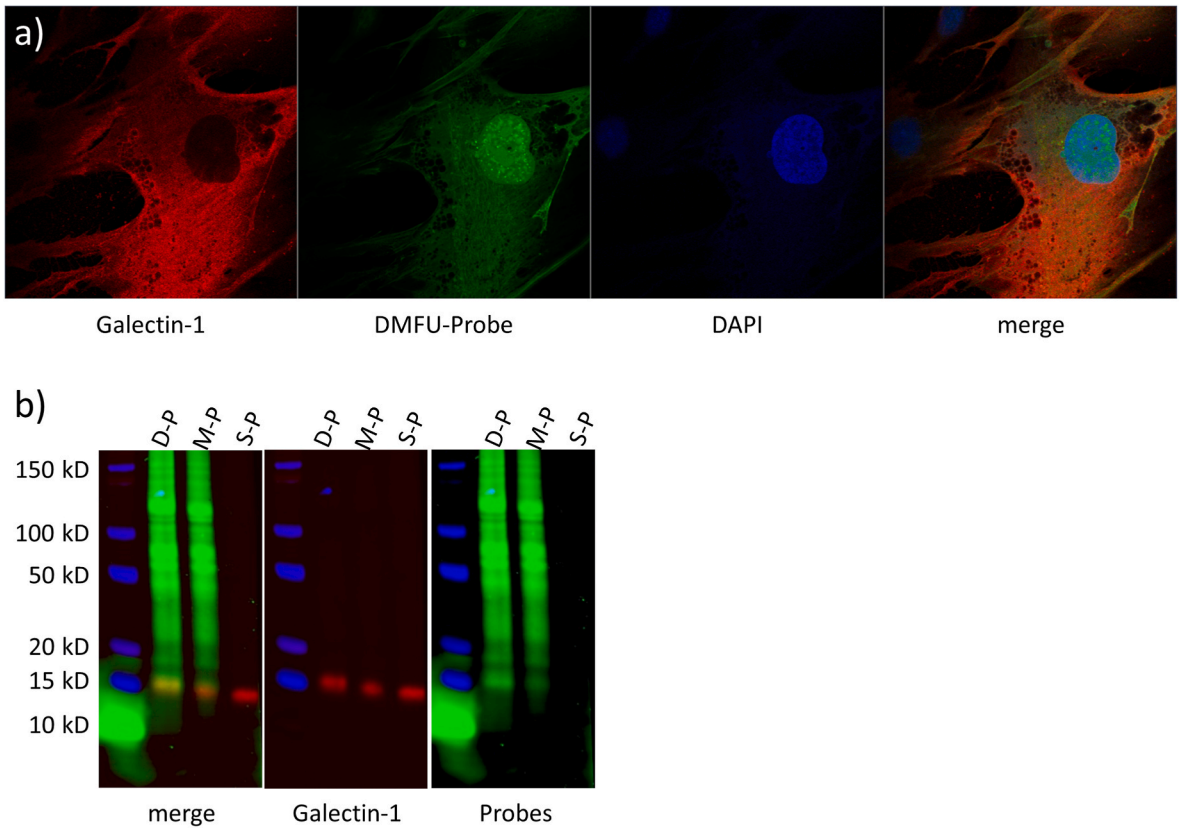

Fig. 6. DMFU and MMFU modify galectin-1. (a) HCASMC treated with DMFU-P (100 μM, 15 min) were clicked to Alexa-488 azide (green fluorescence) resulting in widespread whole cell fluorescence. Counter-imaging for galectin-1 using an anti-galectin-1 antibody and (red) fluorescent secondary antibody revealed diffuse co-localization of DMFU-P targets and galectin-1 in the cytosol. (b) DMFU-P, MMFU-P or succinate-P treated HCASMC (100 μM, 4 h) were lysed, and the modified proteins clicked to the Alexa-488 azide, before being separated by running on a SDS-PAGE gel. Subsequent Western blotting after transfer to a membrane revealed a large number of DMFU-P (D–P) and MMFU-P (M–P) modified proteins (green). One of these bands towards the bottom of the membrane (at ~15 kDa) co-localized with the band recognized by the anti-galectin-1 antibody (red band).

3 (DMFU) or 2 (MMFU) of the 6 Cys residues present in the protein sequence (C42, C60 and C88 for DMFU, C42 and C88 for MMFU) (Fig. 7b and c; Supplementary Fig. 3). No modifications were detected at the other two remaining Cys residues (C2, C16). The peptide containing the remaining Cys (C130) was not detected in the LC-MS dataset, so modification at this position could not be assessed. Additional LC-MS studies, carried out with lower concentrations of DMFU (25 μM, 24 h) revealed that C88 was the only site modified on galectin-1 in HCASMC lysates (as Section 3.4) under these conditions, indicating that this Cys is the most reactive residue with DMFU. Similar studies with MMFU did not detect any modified Cys residues at this lower electrophile concentration.

3.6. LC-MS analysis shows that galectin-1 knockdown and DMFU/MMFU treatment affect many of the same proteins

To examine the functional effects of DMFU- and MMFU-induced modifications (25 μM, 24 h) on cell proteins, LC-MS proteomic analyses were carried out on untreated and treated cells, together with cells in which galectin-1 had been knocked down by siRNA (Fig. 8a, Supplementary Fig. 4). These analyses, which identified ~7600 proteins, showed that HCASMC treated with DMFU showed 25 differentially abundant proteins when compared to untreated control cells, using a 2-fold change cut-off level, and a false discovery rate (FDR) adjusted p value of <0.01 (Fig. 8b, see Supplementary Table 3 for identifications). Analogous experiments with MMFU resulted in the detection of 10 differentially abundant proteins (Fig. 8b, Supplementary Table 3). This lower number is consistent with lower reactivity of this compound. In contrast, galectin-1 knockdown affected ~100 proteins when compared to untreated cells (Fig. 8b, Supplementary Table 3). Interestingly, 12 (~50%) of DMFU differentially abundant proteins, and 8 (80%) of the MMFU differentially abundant proteins were also influenced by galectin-1 knockdown (Fig. 8c). A complete list of affected proteins is presented in Supplementary Table 2. A Fisher's exact test calculation provides an odds ratio for this effect of 1:79 for DMFU, and 1:326 for MMFU. These data therefore indicate that galectin-1 knockdown and DMFU/MMFU treatment affect many of the same cellular targets, though knockdown has a greater influence, as might be expected by the higher degree of protein modification induced by knockdown compared to adduct formation.

These experiments were subsequently extended to examine how galectin-1 knockdown affected the differential expression of proteins induced by DMFU/MMFU treatments, and therefore whether galectin-1 is likely to be important for the mechanisms of action of DMFU and MMFU. These data showed that the changes in abundance induced by DMFU/MMFU were lost when galectin-1 was knocked down. Thus, HCASMC treated with DMFU (25 μM, 24 h) displayed, for example, a 70% reduction in the abundance of ATP Synthase F1 subunit epsilon (ATP5F1E), with this reduction being lost when the cells employed in the experiment were knocked down for galectin-1 (Fig. 8d, Supplementary Fig. 5). Similarly, MMFU reduced the level of ATP5F1E by around 55%, with this effect being lost in galectin-1 knocked down cells (Fig. 8d, Supplementary Fig. 5).

4. Discussion

DMFU and MMFU are both effective drugs for the treatment of

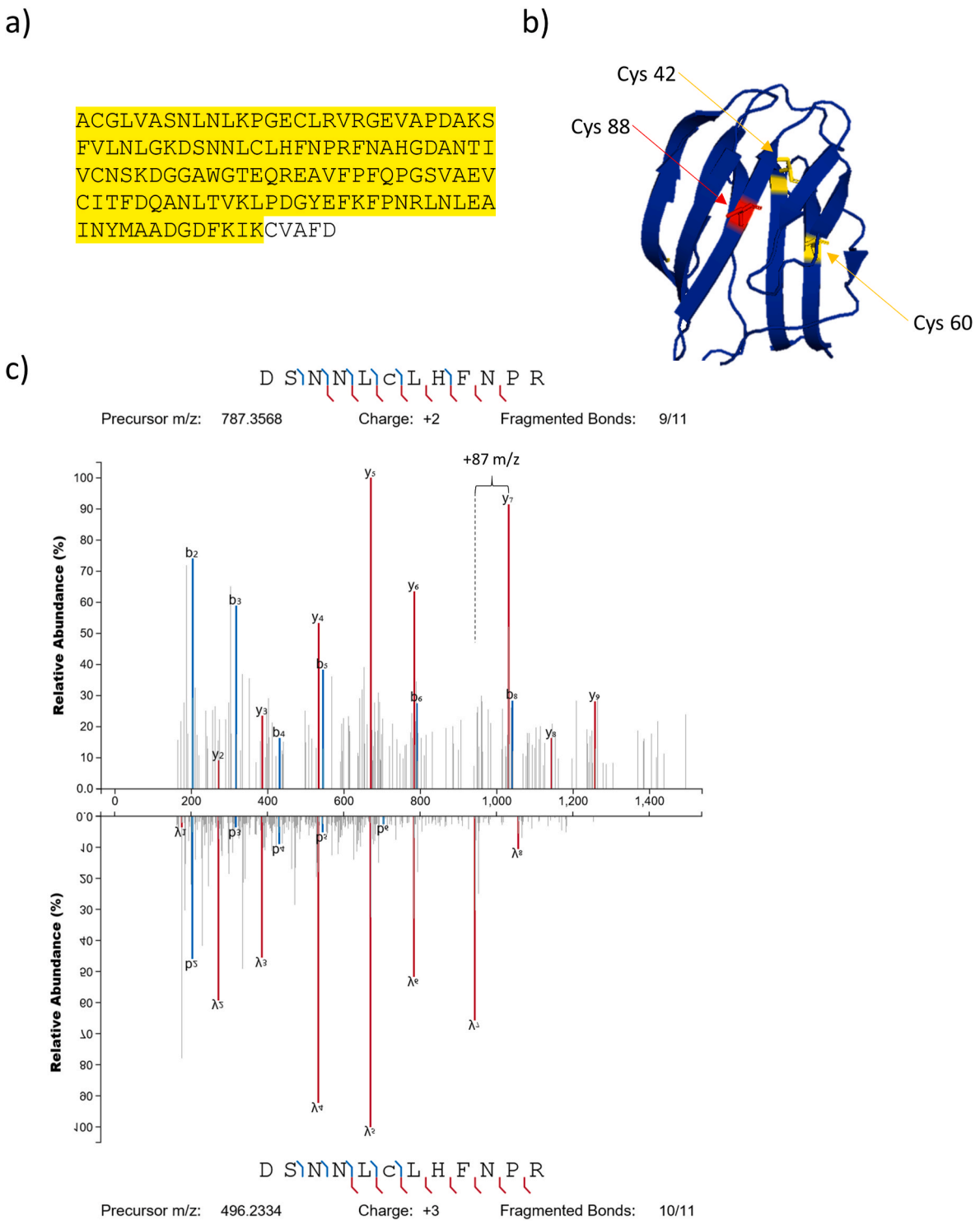

Fig. 7. DMFU and MMFU modify recombinant human galectin-1 protein. (a) LC-MS proteomic analysis (see Materials and methods) detected peptides (highlighted in yellow) covering 96% of the expected protein sequence, with only a small peptide (containing C130) from the carboxyl terminus not observed. (b) Analysis of the peptide dataset with Skyline (v21.2) revealed modifications at three cysteines (C42, C60, C88, indicated in yellow and red) for the reactions with DMFU, and two cysteine (C42, C88) for MMFU. HCASMC treated with 25 μM DMFU for 24 h revealed galectin-1 modified at C88 (indicated in red). (c) Example spectra of a DMFU-modified peptide containing C42 (top spectrum) compared to the same but unmodified peptide presented as a mirror image to allow easy comparison of the spectra. The +87 Da mass shift visible for the y_7 ion corresponds to the expected mass difference between the DMFU adduct (+144.04) and the carbamidomethyl adduct (+57.02, arising from the reduction and alkylation protocol). These data confirm the presence of a DMFU adduct modification at the C42 site. (For interpretation of the references to color in this figure legend, the reader is referred to the Web version of this article.)

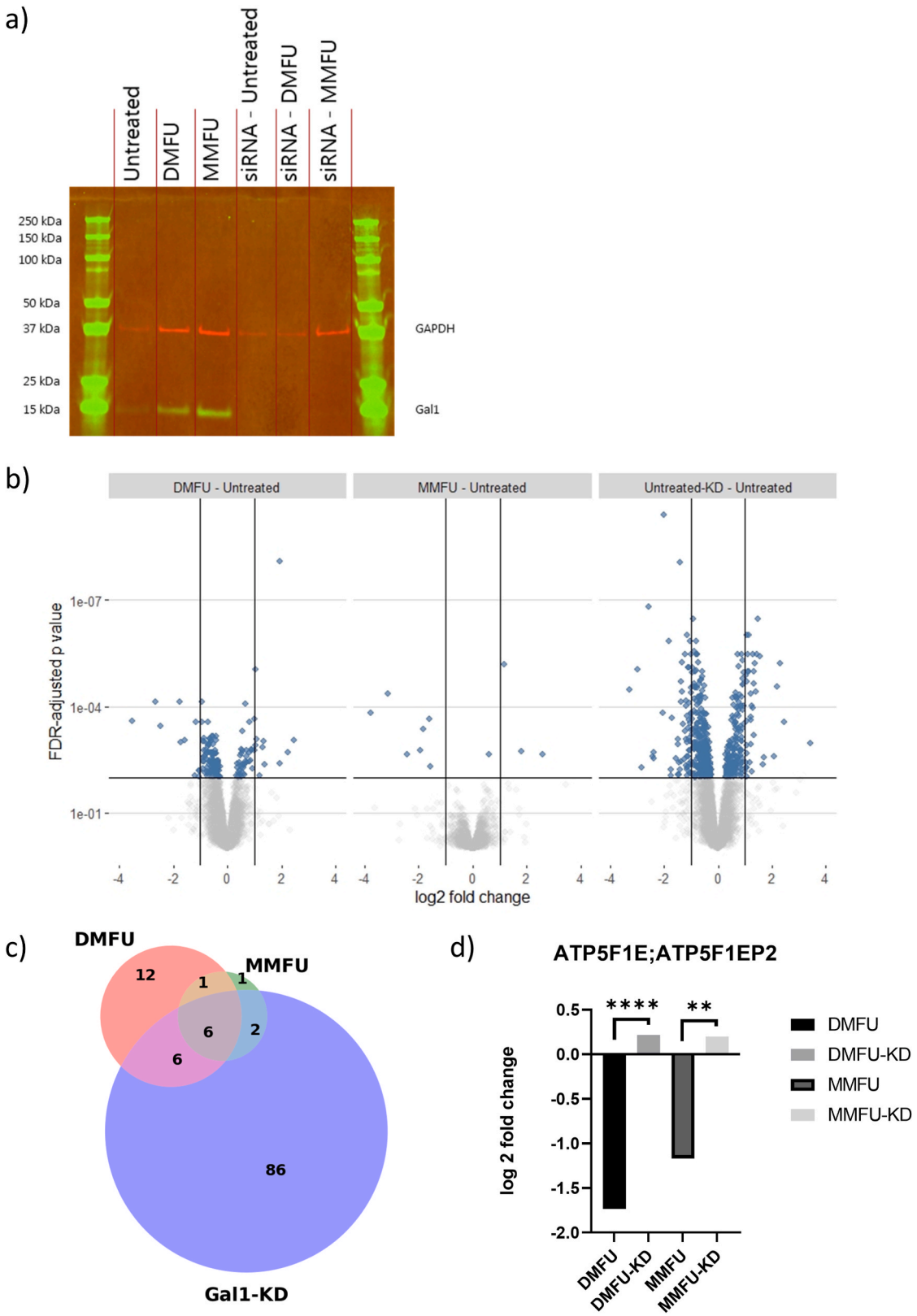

Fig. 8. DMFU, MMFU and galectin-1 influence the abundance of similar proteins. (a) Galectin-knockdown (see Materials and methods) was shown to reduce the concentration of this protein in HCASMC over the course of 5 days. (b) Volcano plots of LC-MS peptide data from DMFU- or MMFU- treated HCASMC (25 μM, 24 h) reveals that DMFU treatment differentially influences the abundance of 25 proteins, and MMFU treatment differentially influences the abundance of 10 proteins when compared to untreated controls. Galectin-1 knockdown influenced 100 proteins. Peptides and hence proteins were determined to be differentially expressed when they had a log2 fold change >1 or < −1, with a false discovery rate-adjusted p-value of <0.01. (c) A Venn-diagram derived from the volcano plots reveals that many of the proteins affected by DMFU and MMFU are also affected by galectin-1 knockdown. The experiment identified ~7600 proteins in total. (d) Example of a protein that was shown to be differentially abundant after HCASMC treatment with DMFU and MMFU. The downregulation of this protein by DMFU and MMFU was not detected in the galectin-1 knockdown cells. The full dataset is presented in the Supplementary data.

psoriasis and multiple sclerosis [1,2]. There is also significant interest in repurposing these drugs for use in other inflammatory diseases including atherosclerosis and Alzheimer's disease [6]. However, the exact molecular actions of DMFU and MMFU remain to be fully uncovered, though it is likely that this occurs via the modification of Cys residues on proteins. It is however also possible that adduction may also occur at other nucleophilic sites (e.g the amine groups of DNA and RNA bases) though the kinetics of such reactions appear to be much slower. However, if it is assumed that Cys residues are the major effectors of DMFU/MMFU actions, the question remains as to which of the very large number of these residues are responsible for their biological action. The limited specificity of DMFU and MMFU (as revealed here and previously [15,22]) makes this both a key and challenging question. Identification of the causal events would allow data-driven design of new drugs with increased specificity and potency, and decreased off-target effects.

Keap1, p63, GAPDH, Irak4, and cofilin have all been previously identified as targets of DMFU or MMFU [20–23], with this resulting in the hypothesis that DMFU/MMFU react with key Cys residue in these proteins, and alteration (inhibition) of their activity. Such inhibition is expected to have anti-inflammatory effects. Thus, adduction at Cys151 (or other Cys residues) on Keap1 is proposed to result in decreased ubiquitination and proteasomal degradation of NRF2, allowing newly-synthesized NRF2, which is regarded as a master regulator, to translocate to the nucleus, and upregulate protective genes [37]. Similarly, inhibition of GAPDH is likely to limit ATP production in activated immune cells [20], and inhibition of Irak4 has been reported to inhibit pro-inflammatory signal transduction during T-cell activation [21]. Although, Keap1 is by far the most discussed target, some data do not support a key role for this species [15,24,25,27,38]. Furthermore, Keap1 has not been previously identified in non-targeted proteomic studies that have examined DMFU/MMFU modifications [15,28,29].

In the work reported here, we have utilized alkyne-modified versions of DMFU and MMFU (and the corresponding succinate species, as a negative control) to identify the DMFU/MMFU sensitive proteome in an unbiased manner. As addition of the alkyne tag might perturb the chemical and biological properties of the compounds, both kinetic analyses and cellular experiments (viability and gene induction), have been carried out to examine possible differences in behavior. All of the reported data support the conclusion that the probes behave in a similar manner to the parent drugs, indicating that the alkyne-tagged probes accurately report on DMFU/MMFU-induced effects.

A pull-down of DMFU-P or MMFU-P adducted proteins revealed that DMFU and MMFU are poorly specific compounds with adduction detected with hundreds of different proteins (Fig. 5 and Supplementary Table 2). The MS data includes many of the previously hypothesized targets of DMFU/MMFU, including Keap1, GAPDH, and cofilin. These data therefore support the hypothesis that these proteins are biological targets of DMFU or MMFU. The current dataset also shows some overlap in targets with other datasets. Thus, we have detected voltage-dependent anion-selective channel protein 2 (VDAC2) as one of the top targets in the MMFU data set; this protein has been identified previously as being highly reactive towards fumarates [21]. The same is true for S100A6 protein, vimentin, and thioredoxin, amongst others [28]. However, the most intense hit in our dataset for DMFU-P and MMFU-P was galectin-1, and therefore further studies focused on this species. It should however be noted that string database analysis (Fig. 5b) of the top 10 DMFU-probe hits reveals many of the top hits are closely linked in this analyses, potentially indicating significant interactions or complex formation, which may result in aberrant quantification data, and an over-emphasis on such proteins in the dataset. The stringent and extensive washing procedure should minimize these effects, as this would have been expected to dissociate all but the most tight binding, and the low number of 'background' hits detected with the succinate probe suggests that such artefacts may be minimal.

There is substantial evidence in the literature to support the hypothesis that galectin-1 is a significant immune regulator, thus the adduct formation detected here on this protein, may explain some of the observed biological effects of these drugs. This β-galactoside carbohydrate binding protein [39] has established immune modulatory functions especially with regard to T-cell driven autoimmunity [40–43]. Galectin-1 has been shown to reduce interleukin-12 release [44], and to drive macrophages towards an anti-inflammatory (M2) isotype [45,46]. It is known to induce apoptosis in TH1 or TH17 cells, and to increase clearance of leukocytes by phagocytosis [43,47]. Of major importance is the observation that galectin-1 is a redox-sensitive protein, with the above actions dependent on the protein being in a reduced state [48]. Thus galectin-1 can exist with both reduced and oxidized Cys residues, with the thiol groups of the Cys residues converted to disulfides by oxidants, which have been shown to be generated at elevated levels in many pathologies including both multiple sclerosis and psoriasis [49–52]. An intra-chain disulfide formation between C16 and C88 appears to be of particular importance [48]. This oxidative switch from free C16 and C88 to a disulfide between these residues has been reported to negate much of the anti-inflammatory actions of galectin-1. Thus, inhibition of disulfide bond formation, by site-directed mutation of C16 or C88 to a Ser residue (i.e. C16 or C88 → S16/S88) renders galectin-1 anti-inflammatory, even under conditions of oxidative stress [48]. A summary of the proposed effects of DMFU/MMFU on galectin-1 and its biological activity is presented in Fig. 9.

Our data show that DMFU and MMFU can modify at least four of the six (and possibly 5, as C130 was not detected) galectin-1 Cys residues (Fig. 7). Of these residues, C88 appears to be the most sensitive, as this was the only one detected as a modified species with low levels of DMFU in HCASMC lysates. The formation of an adduct at this residue would be expected to prevent the formation of the C16–C88 disulfide, and thereby prevent the formation of the inhibitory intra-chain disulfide bond. The DMFU-adducted species would therefore be maintained in its anti-inflammatory form. Galectin-1 knockdown in the HCASMC was used to test the hypothesis that galectin-1 is important for the actions of DMFU and MMFU. Comparison of the cell populations showed that HCASMC treated with DMFU had 25 differentially abundant proteins (DAPs), MMFU treatment yielded 10 DAPs, and the galectin-1 knockdown 100 DAPs. Interestingly, the proteins that were differentially abundant after DMFU or MMFU treatment showed a strong crossover with those affected by galectin-1 knockdown (Fig. 8). This suggests that the actions of galectin-1 and the two fumarates are closely connected. Thus, the ATPase subunit ATP5F1E was downregulated by both DMFU and MMFU, but the galectin-1 knocked down cells failed to show this change, suggesting that this change is reliant on the presence of galectin-1 (Fig. 8d). As galectin-1 is involved in cell signaling, relatively modest levels of DMFU/MMFU-modified galectin-1 may have a significant biological effect and this possibility is currently under study. Other processes or compounds that also stabilize galectin-1 in its reduced (anti-inflammatory) form might also have therapeutic potential in various immune driven diseases.

Many of the previously discussed DMFU/MMFU targets including Keap1, GAPDH, and Irak4 have a common theme of fumarate modification resulting in an inhibitory effect. Thus, DMFU/MMFU inhibition of GAPDH has been proposed to limit the energy sources available for activated immune cells, resulting in decreased inflammation [20]. However, it might be expected that extensive GAPDH modification would be needed to induce such a change, and it is unclear whether such massive modification is biologically realistic, and especially in the light of the current data that indicate that DMFU and MMFU affect a large number of alternative targets. This may not be the case for highly (kinetically favored) targets such as Keap1, but this does not appear to be the case for GAPDH on the basis of our previous kinetic data [13]. In contrast, galectin-1 modification by DMFU/MMFU is proposed to act via a stabilizing process (prevention of disulfide bond formation) and can therefore be considered as an activating modification.

A number of other proteins identified in the current study including

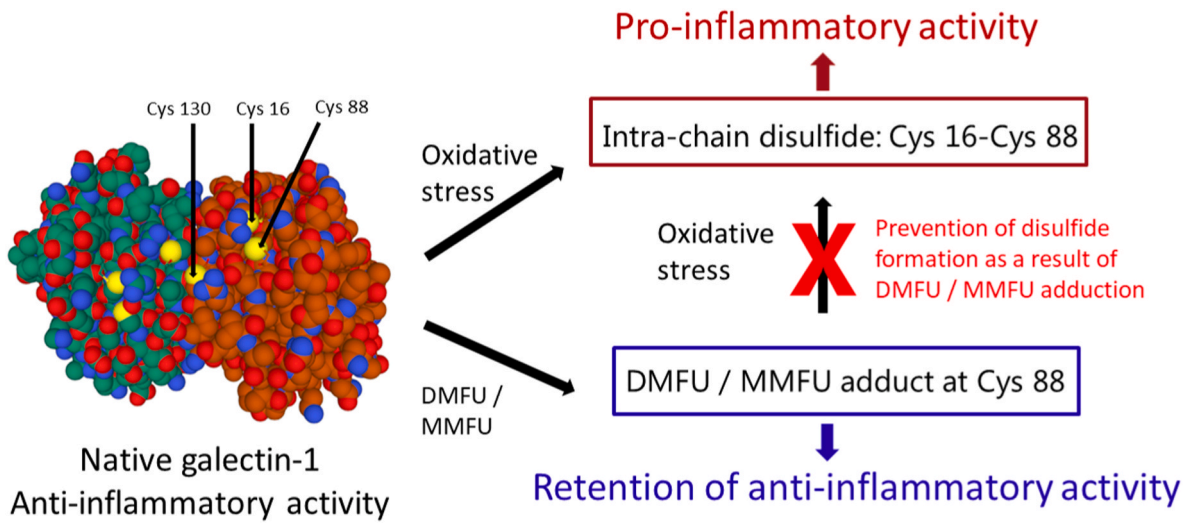

Fig. 9. Proposed mechanism by which DMFU/MMFU adduction may modulate galectin-1 activity. A rendering of the 3-dimensional structure of galectin-1 (from PDB structure 1w6n) is presented, with this containing two protein chains (green and brown respectively, with nitrogen atoms in blue, oxygen atoms in red and sulfur atoms in yellow). The locations of three of the Cys residues (from 6 in total) are indicated together with their sequence positions. Cys 16 and Cys 88 are reported to form a disulfide bond on exposure to the oxidants generated during the development of multiple sclerosis or psoriasis (see text). This process is proposed to convert the anti-inflammatory parent protein to an inactive or pro-inflammatory isoform. Of these two Cys residues, Cys 88 appears to have a greater solvent accessibility, consistent with a greater susceptibility to adduct formation with DMFU and MMFU. The formation of these adduct species prevents formation of the disulfide bond (as Cys 88 is adducted with the drug), and is proposed to lock or retain the protein in its anti-inflammatory form, resulting in the reported positive effects of DMFU or MMFU in these two diseases.

Annexin A1 (also known as lipocortin-1), Park7 (also known as DJ-1), PCBP1 (Poly(rC)-binding protein 1) and MXRA7 (matrix remodeling associated 7) have been linked with either multiple sclerosis (and the murine experimental autoimmune encephalomyelitis, EAE, model), or psoriasis. Thus there is abundant evidence for elevated levels of Annexin A1 in both human multiple sclerosis plaques [53–55], and the brains of mice [56,57] and rats [58] with EAE, with the levels of this protein being strongly and positively associated with disease severity. Although considerable data indicates that this protein can have anti-inflammatory actions [53], other data have been presented indicating that Annexin A1 null mice have a decreased development of EAE [56], suggesting that this protein has complex biological effects. The current data indicating that DMFU and MMFU target the Cys residues on this protein, may indicate that adduction at these sites may mimic the positive effects of Annexin A1 knockdown, and may support the hypothesis that reducing Annexin A1 activity or expression can have positive effects in multiple sclerosis [56].

Evidence has also been presented that modification of the Cys residues (and particularly Cys-106) of Park 7/DJ-1 can modulate the cellular localization of the protein and its biological activity [59,60], with oxidation of the Cys residue giving a more acidic isoform that translocates to mitochondria [61,62]. This probably arises from the formation of a sulfinic acid from the thiol [61] (though other oxy acids may also be generated). Strong evidence links elevated levels of Park 7/DJ-1 with multiple sclerosis lesions, but whether this is a causal or associative effect is less clear [59,60,63]. Whether DMFU/MMFU modify Park 7/DJ-1 at the same sites and induce similar biological effects remains to be established, though if adduction does occur at Cys-106, the chemical structure of the resulting adduct would clearly be different to that induced by oxidation. It is also of interest to note that Park 7/DJ-1 and NRF2 appear to be regulated as least partly in synchrony [60], with NRF2 stabilized by Park 7/DJ-1 [64]. Thus, the effects of DMFU/MMFU on Keap1 and Park 7/DJ-1, may act in synchrony to enhance expression of protective NRF2-dependent genes.

Data on the potential roles, and effects of modulation by DMFU and MMFU of MXRA7 and PCBP1, and the effects of this on psoriasis [65] and EAE [66] with which these two proteins have been associated is unclear. MXRA7-deficient mice have been reported to develop more severe disease [65], indicating that this protein acts as a negative regulator of disease development, and therefore inhibition of the function of this protein by DMFU/MMFU may mimic the deletion of this protein. The effects of PCBP1 in EAE [66] have been reported to be linked with iron status, with iron deficiency resulting in increased caspase-dependent proteolysis of PCBP1, decreased levels of granulocyte-macrophage colony stimulating factor (GM-CSF) and other pro-inflammatory cytokine production, and decreased EAE. Whether and how DMFU/MMFU may affect this pathway is unclear.

In conclusion, the data reported in this study indicate that alkyne-tagging of electrophiles and subsequent use of click-chemistry to allow enrichment and identification of drug targets by proteomic approaches is a powerful and unbiased method to identify cellular targets. In particular, the use of these DMFU- and MMFU-probes has allowed identification of a very large number of additional of cellular proteins whose Cys residues are targets for alpha,beta-unsaturated carbonyls via Michael adduction reactions.

Declaration of competing interests

MJD declares consultancy contracts with Novo Nordisk A/S. This funder had no role in the design of the study; in the collection, analyses, or interpretation of data; in the writing of the manuscript, or in the decision to publish the results. The other authors declare no conflict of interest.

Data availability

Data will be made available on request.

Acknowledgements

This work was supported by grants from the Novo Nordisk Foundation (NNF13OC0004294 and NNF20SA0064214 to MJD), and a Lundbeck Foundation Fellowship (102–6816/20-3000) to LFG.

Appendix A. Supplementary data

Supplementary data to this article can be found online at https://doi.org/10.1016/j.redox.2022.102560.

References

[1] J.M. Burton, P. O'Connor, Novel oral agents for multiple sclerosis, Curr. Neurol. Neurosci. Rep. 7 (3) (2007) 223–230.

[2] A.A. Berger, E.R. Sottosanti, A. Winnick, J. Izygon, K. Berardino, E.M. Cornett, A. D. Kaye, G. Varrassi, O. Viswanath, I. Urits, Monomethyl fumarate (MMF, bafiertam) for the treatment of relapsing forms of multiple sclerosis (MS), Neurol. Int. 13 (2) (2021) 207–223.

[3] M. Luo, Q. Sun, H. Zhao, J. Tao, D. Yan, The effects of dimethyl fumarate on atherosclerosis in the apolipoprotein E-deficient mouse model with streptozotocin-induced hyperglycemia mediated by the nuclear factor erythroid 2-related factor 2/antioxidant response element (Nrf2/ARE) signaling pathway, Med. Sci. Mon. Int. Med. J. Exp. Clin. Res. 25 (2019) 7966–7975.

[4] X. Sun, X. Suo, X. Xia, C. Yu, Y. Dou, Dimethyl fumarate is a potential therapeutic option for alzheimer's disease, J Alzheimers Dis 85 (1) (2022) 443–456.

[5] X. Jing, H. Shi, C. Zhang, M. Ren, M. Han, X. Wei, X. Zhang, H. Lou, Dimethyl fumarate attenuates 6-OHDA-induced neurotoxicity in SH-SY5Y cells and in animal model of Parkinson's disease by enhancing Nrf2 activity, Neuroscience 286 (2015) 131–140.

[6] I. Lastres-Becker, A.J. Garcia-Yague, R.H. Scannevin, M.J. Casarejos, S. Kugler, A. Rabano, A. Cuadrado, Repurposing the NRF2 activator dimethyl fumarate as therapy against synucleinopathy in Parkinson's disease, Antioxidants Redox Signal. 25 (2) (2016) 61–77.

[7] Y. Wang, P. Bhargava, Diroximel fumarate to treat multiple sclerosis, Drugs Today 56 (7) (2020) 431–437.

[8] S. Kourakis, C.A. Timpani, J.B. de Haan, N. Gueven, D. Fischer, E. Rybalka, Dimethyl fumarate and its esters: a drug with broad clinical utility? Pharmaceuticals 13 (10) (2020).

[9] M.J. Palte, A. Wehr, M. Tawa, K. Perkin, R. Leigh-Pemberton, J. Hanna, C. Miller, N. Penner, Improving the gastrointestinal tolerability of fumaric acid esters: early findings on gastrointestinal events with diroximel fumarate in patients with relapsing-remitting multiple sclerosis from the phase 3, open-label EVOLVE-MS-1 study, Adv. Ther. 36 (11) (2019) 3154–3165.

[10] K.E. Attfield, L.T. Jensen, M. Kaufmann, M.A. Friese, L. Fugger, The immunology of multiple sclerosis, Nat. Rev. Immunol. 22 (12) (2022) 734–750, https://doi.org/10.1038/s41577-022-00718-z.

[11] E. von Stebut, K. Reich, D. Thaci, W. Koenig, A. Pinter, A. Korber, T. Rassaf, A. Waisman, V. Mani, D. Yates, J. Frueh, C. Sieder, N. Melzer, N.N. Mehta, T. Gori, Impact of secukinumab on endothelial dysfunction and other cardiovascular disease parameters in psoriasis patients over 52 weeks, J. Invest. Dermatol. 139 (5) (2019) 1054–1062.

[12] M. Marovt, P.B. Marko, M. Pirnat, R. Ekart, Effect of biologics targeting interleukin-23/-17 axis on subclinical atherosclerosis: results of a pilot study, Clin. Exp. Dermatol. 45 (5) (2020) 560–564.

[13] M. Sauerland, R. Mertes, C. Morozzi, A.L. Eggler, L.F. Gamon, M.J. Davies, Kinetic assessment of Michael addition reactions of alpha, beta-unsaturated carbonyl compounds to amino acid and protein thiols, Free Radic. Biol. Med. 169 (2021) 1–11.

[14] J.A. Ward, A. Pinto-Fernandez, L. Cornelissen, S. Bonham, L. Diaz-Saez, O. Riant, K.V.M. Huber, B.M. Kessler, O. Feron, E.W. Tate, Re-evaluating the mechanism of action of alpha,beta-unsaturated carbonyl DUB inhibitors b-AP15 and VLX1570: a paradigmatic example of unspecific protein cross-linking with Michael acceptor motif-containing drugs, J. Med. Chem. 63 (7) (2020) 3756–3762.

[15] M.M. Blewett, J. Xie, B.W. Zaro, K.M. Backus, A. Altman, J.R. Teijaro, B.F. Cravatt, Chemical proteomic map of dimethyl fumarate-sensitive cysteines in primary human T cells, Sci. Signal. 9 (445) (2016) rs10.

[16] I. Kastrati, M.I. Siklos, E.L. Calderon-Gierszal, L. El-Shennawy, G. Georgieva, E. N. Thayer, G.R. Thatcher, J. Frasor, Dimethyl fumarate inhibits the nuclear factor kappaB pathway in breast cancer cells by covalent modification of p65 protein, J. Biol. Chem. 291 (7) (2016) 3639–3647.

[17] T. Rantanen, The cause of the Chinese sofa/chair dermatitis epidemic is likely to be contact allergy to dimethylfumarate, a novel potent contact sensitizer, Br. J. Dermatol. 159 (1) (2008) 218–221.

[18] E.L. Mills, D.G. Ryan, H.A. Prag, D. Dikovskaya, D. Menon, Z. Zaslona, M. P. Jedrychowski, A.S.H. Costa, M. Higgins, E. Hams, J. Szpyt, M.C. Runtsch, M. S. King, J.F. McGouran, R. Fischer, B.M. Kessler, A.F. McGettrick, M.M. Hughes, R. G. Carroll, L.M. Booty, E.V. Knatko, P.J. Meakin, M.L.J. Ashford, L.K. Modis, G. Brunori, D.C. Sevin, P.G. Fallon, S.T. Caldwell, E.R.S. Kunji, E.T. Chouchani, C. Frezza, A.T. Dinkova-Kostova, R.C. Hartley, M.P. Murphy, L.A. O'Neill, Itaconate is an anti-inflammatory metabolite that activates Nrf2 via alkylation of KEAP1, Nature 556 (7699) (2018) 113–117.

[19] J. Muri, H. Wolleb, P. Broz, E.M. Carreira, M. Kopf, Electrophilic Nrf2 activators and itaconate inhibit inflammation at low dose and promote IL-1beta production and inflammatory apoptosis at high dose, Redox Biol. 36 (2020), 101647.

[20] M.D. Kornberg, P. Bhargava, P.M. Kim, V. Putluri, A.M. Snowman, N. Putluri, P. A. Calabresi, S.H. Snyder, Dimethyl fumarate targets GAPDH and aerobic glycolysis to modulate immunity, Science 360 (6387) (2018) 449–453.

[21] B.W. Zaro, E.V. Vinogradova, D.C. Lazar, M.M. Blewett, R.M. Suciu, J. Takaya, S. Studer, J.C. de la Torre, J.L. Casanova, B.F. Cravatt, J.R. Teijaro, Dimethyl fumarate disrupts human innate immune signaling by targeting the IRAK4-MyD88 complex, J. Immunol. 202 (9) (2019) 2737–2746.

[22] G.G. Piroli, A.M. Manuel, T. Patel, M.D. Walla, L. Shi, S.A. Lanci, J. Wang, A. Galloway, P.I. Ortinski, D.S. Smith, N. Frizzell, Identification of novel protein targets of dimethyl fumarate modification in neurons and astrocytes reveals actions independent of Nrf2 stabilization, Mol. Cell. Proteomics 18 (3) (2019) 504–519.

[23] K. Takaya, T. Suzuki, H. Motohashi, K. Onodera, S. Satomi, T.W. Kensler, M. Yamamoto, Validation of the multiple sensor mechanism of the Keap1-Nrf2 system, Free Radic. Biol. Med. 53 (4) (2012) 817–827.

[24] K. Kobayashi, H. Tomiki, Y. Inaba, M. Ichikawa, B.S. Kim, C.S. Koh, Dimethyl fumarate suppresses Theiler's murine encephalomyelitis virus-induced demyelinating disease by modifying the Nrf2-Keap1 pathway, Int. Immunol. 27 (7) (2015) 333–344.

[25] R.A. Linker, D.H. Lee, S. Ryan, A.M. van Dam, R. Conrad, P. Bista, W. Zeng, X. Hronowsky, A. Buko, S. Chollate, G. Ellrichmann, W. Bruck, K. Dawson, S. Goelz, S. Wiese, R.H. Scannevin, M. Lukashev, R. Gold, Fumaric acid esters exert neuroprotective effects in neuroinflammation via activation of the Nrf2 antioxidant pathway, Brain 134 (Pt 3) (2011) 678–692.

[26] S. Unni, P. Deshmukh, G. Krishnappa, P. Kommu, B. Padmanabhan, Structural insights into the multiple binding modes of Dimethyl Fumarate (DMF) and its analogs to the Kelch domain of Keap1, FEBS J. 288 (5) (2021) 1599–1613, https://doi.org/10.1111/febs.15485.

[27] U. Schulze-Topphoff, M. Varrin-Doyer, K. Pekarek, C.M. Spencer, A. Shetty, S. A. Sagan, B.A. Cree, R.A. Sobel, B.T. Wipke, L. Steinman, R.H. Scannevin, S. S. Zamvil, Dimethyl fumarate treatment induces adaptive and innate immune modulation independent of Nrf2, Proc. Natl. Acad. Sci. U. S. A. 113 (17) (2016) 4777–4782.

[28] E.D. Merkley, T.O. Metz, R.D. Smith, J.W. Baynes, N. Frizzell, The succinated proteome, Mass Spectrom. Rev. 33 (2) (2014) 98–109.

[29] M. Yang, N. Ternette, H. Su, R. Dabiri, B.M. Kessler, J. Adam, B.T. Teh, P.J. Pollard, The succinated proteome of FH-mutant tumours, Metabolites 4 (3) (2014) 640–654.

[30] M.B. Sauerland, M.J. Davies, Electrophile versus oxidant modification of cysteine residues: kinetics as a key driver of protein modification, Arch. Biochem. Biophys. (2022), 109344.

[31] C. Morozzi, M. Sauerland, L.F. Gamon, A. Manandhar, T. Ulven, M.J. Davies, Synthesis and cellular evaluation of click-chemistry probes to study the biological effects of alpha, beta-unsaturated carbonyls, Redox Biol. 52 (2022), 102299.

[32] M. Tong, S. Suttapitugsakul, R. Wu, Effective method for accurate and sensitive quantitation of rapid changes of newly synthesized proteins, Anal. Chem. 92 (14) (2020) 10048–10057.

[33] B. Schwanhausser, D. Busse, N. Li, G. Dittmar, J. Schuchhardt, J. Wolf, W. Chen, M. Selbach, Global quantification of mammalian gene expression control, Nature 473 (7347) (2011) 337–342.

[34] J. Bruck, R. Dringen, A. Amasuno, I. Pau-Charles, K. Ghoreschi, A review of the mechanisms of action of dimethylfumarate in the treatment of psoriasis, Exp. Dermatol. 27 (6) (2018) 611–624.

[35] H.C. Kolb, M.G. Finn, K.B. Sharpless, Click chemistry: diverse chemical function from a few good reactions, Angew. Chem., Int. Ed. 40 (11) (2001) 2004–2021.

[36] C.W. Tornoe, C. Christensen, M. Meldal, Peptidotriazoles on solid phase: [1,2,3]-triazoles by regiospecific copper(i)-catalyzed 1,3-dipolar cycloadditions of terminal alkynes to azides, J. Org. Chem. 67 (9) (2002) 3057–3064.

[37] M.S. Brennan, M.F. Matos, B. Li, X. Hronowski, B. Gao, P. Juhasz, K.J. Rhodes, R. H. Scannevin, Dimethyl fumarate and monoethyl fumarate exhibit differential effects on KEAP1, NRF2 activation, and glutathione depletion in vitro, PLoS One 10 (3) (2015), e0120254.

[38] G.O. Gillard, B. Collette, J. Anderson, J. Chao, R.H. Scannevin, D.J. Huss, J. D. Fontenot, DMF, but not other fumarates, inhibits NF-kappaB activity in vitro in an Nrf2-independent manner, J. Neuroimmunol. 283 (2015) 74–85.

[39] H. Verkerke, M. Dias-Baruffi, R.D. Cummings, C.M. Arthur, S.R. Stowell, Galectins: an ancient family of carbohydrate binding proteins with modern functions, Methods Mol. Biol. 2442 (2022) 1–40.

[40] C.M. Arthur, L.C. Rodrigues, M.D. Baruffi, H.C. Sullivan, R.D. Cummings, S. R. Stowell, Detection of phosphatidylserine exposure on leukocytes following treatment with human galectins, Methods Mol. Biol. 1207 (2015) 185–200.

[41] G. Levi, R. Tarrab-Hazdai, V.I. Teichberg, Prevention and therapy with electrolectin of experimental autoimmune myasthenia gravis in rabbits, Eur. J. Immunol. 13 (6) (1983) 500–507.

[42] L. Santucci, S. Fiorucci, F. Cammilleri, G. Servillo, B. Federici, A. Morelli, Galectin-1 exerts immunomodulatory and protective effects on concanavalin A-induced hepatitis in mice, Hepatology 31 (2) (2000) 399–406.

[43] M.A. Toscano, G.A. Bianco, J.M. Ilarregui, D.O. Croci, J. Correale, J.D. Hernandez, N.W. Zwirner, F. Poirier, E.M. Riley, L.G. Baum, G.A. Rabinovich, Differential glycosylation of TH1, TH2 and TH-17 effector cells selectively regulates susceptibility to cell death, Nat. Immunol. 8 (8) (2007) 825–834.

[44] H. Yaseen, S. Butenko, I. Polishuk-Zotkin, S. Schif-Zuck, J.M. Perez-Saez, G. A. Rabinovich, A. Ariel, Galectin-1 facilitates macrophage reprogramming and resolution of inflammation through IFN-beta, Front. Pharmacol. 11 (2020) 901.

[45] R. Rostoker, H. Yaseen, S. Schif-Zuck, R.G. Lichtenstein, G.A. Rabinovich, A. Ariel, Galectin-1 induces 12/15-lipoxygenase expression in murine macrophages and favors their conversion toward a pro-resolving phenotype, Prostag. Other Lipid Mediat. 107 (2013) 85–94.

[46] M.A. Toscano, A.G. Commodaro, J.M. Ilarregui, G.A. Bianco, A. Liberman, H. M. Serra, J. Hirabayashi, L.V. Rizzo, G.A. Rabinovich, Galectin-1 suppresses autoimmune retinal disease by promoting concomitant Th2- and T regulatory-mediated anti-inflammatory responses, J. Immunol. 176 (10) (2006) 6323–6332.

[47] M. Dias-Baruffi, H. Zhu, M. Cho, S. Karmakar, R.P. McEver, R.D. Cummings, Dimeric galectin-1 induces surface exposure of phosphatidylserine and phagocytic recognition of leukocytes without inducing apoptosis, J. Biol. Chem. 278 (42) (2003) 41282–41293.
[48] M.M. Fettis, G.A. Hudalla, Engineering reactive oxygen species-resistant galectin-1 dimers with enhanced lectin activity, Bioconjugate Chem. 29 (7) (2018) 2489–2496.
[49] A. Signorile, A. Ferretta, M. Ruggieri, D. Paolicelli, P. Lattanzio, M. Trojano, D. De Rasmo, Mitochondria, oxidative stress, cAMP signalling and apoptosis: a crossroads in lymphocytes of multiple sclerosis, a possible role of nutraceutics, Antioxidants 10 (1) (2020).
[50] T.O. Tobore, Oxidative/nitroxidative stress and multiple sclerosis, J. Mol. Neurosci. 71 (3) (2021) 506–514.
[51] C.C. Chiang, W.J. Cheng, M. Korinek, C.Y. Lin, T.L. Hwang, Neutrophils in psoriasis, Front. Immunol. 10 (2019) 2376.
[52] Q. Zhou, U. Mrowietz, M. Rostami-Yazdi, Oxidative stress in the pathogenesis of psoriasis, Free Radic. Biol. Med. 47 (7) (2009) 891–905.
[53] S. Probst-Cousin, D. Kowolik, K. Kuchelmeister, C. Kayser, B. Neundorfer, D. Heuss, Expression of annexin-1 in multiple sclerosis plaques, Neuropathol. Appl. Neurobiol. 28 (4) (2002) 292–300.
[54] I.A. MacPhee, F.A. Antoni, D.W. Mason, Spontaneous recovery of rats from experimental allergic encephalomyelitis is dependent on regulation of the immune system by endogenous adrenal corticosteroids, J. Exp. Med. 169 (2) (1989) 431–445.
[55] A.J. Elderfield, J. Newcombe, C. Bolton, R.J. Flower, Lipocortins (annexins) 1, 2, 4 and 5 are increased in the central nervous system in multiple sclerosis, J. Neuroimmunol. 39 (1–2) (1992) 91–100.
[56] N. Paschalidis, A.J. Iqbal, F. Maione, E.G. Wood, M. Perretti, R.J. Flower, F. D'Acquisto, Modulation of experimental autoimmune encephalomyelitis by endogenous annexin A1, J. Neuroinflammation 6 (2009) 33.
[57] I. Huitinga, J. Bauer, P.J. Strijbos, N.J. Rothwell, C.D. Dijkstra, F.J. Tilders, Effect of annexin-1 on experimental autoimmune encephalomyelitis (EAE) in the rat, Clin. Exp. Immunol. 111 (1) (1998) 198–204.
[58] C. Bolton, A.J. Elderfield, R.J. Flower, The detection of lipocortins 1, 2 and 5 in central nervous system tissues from Lewis rats with acute experimental allergic encephalomyelitis, J. Neuroimmunol. 29 (1–3) (1990) 173–181.
[59] M. Hirotani, C. Maita, M. Niino, S. Iguchi-Ariga, S. Hamada, H. Ariga, H. Sasaki, Correlation between DJ-1 levels in the cerebrospinal fluid and the progression of disabilities in multiple sclerosis patients, Mult. Scler. 14 (8) (2008) 1056–1060.
[60] J. van Horssen, J.A. Drexhage, T. Flor, W. Gerritsen, P. van der Valk, H.E. de Vries, Nrf2 and DJ1 are consistently upregulated in inflammatory multiple sclerosis lesions, Free Radic. Biol. Med. 49 (8) (2010) 1283–1289.
[61] R.M. Canet-Aviles, M.A. Wilson, D.W. Miller, R. Ahmad, C. McLendon, S. Bandyopadhyay, M.J. Baptista, D. Ringe, G.A. Petsko, M.R. Cookson, The Parkinson's disease protein DJ-1 is neuroprotective due to cysteine-sulfinic acid-driven mitochondrial localization, Proc. Natl. Acad. Sci. U. S. A. 101 (24) (2004) 9103–9108.
[62] H.M. Li, T. Niki, T. Taira, S.M. Iguchi-Ariga, H. Ariga, Association of DJ-1 with chaperones and enhanced association and colocalization with mitochondrial Hsp70 by oxidative stress, Free Radic. Res. 39 (10) (2005) 1091–1099.
[63] N. Lev, D. Ickowicz, Y. Barhum, N. Blondheim, E. Melamed, D. Offen, Experimental encephalomyelitis induces changes in DJ-1: implications for oxidative stress in multiple sclerosis, Antioxidants Redox Signal. 8 (11–12) (2006) 1987–1995.
[64] C.M. Clements, R.S. McNally, B.J. Conti, T.W. Mak, J.P. Ting, DJ-1, a cancer- and Parkinson's disease-associated protein, stabilizes the antioxidant transcriptional master regulator Nrf2, Proc. Natl. Acad. Sci. U. S. A. 103 (41) (2006) 15091–15096.
[65] J. Ning, Y. Shen, T. Wang, M. Wang, W. Liu, Y. Sun, F. Zhang, L. Chen, Y. Wang, Altered expression of matrix remodelling associated 7 (MXRA7) in psoriatic epidermis: evidence for a protective role in the psoriasis imiquimod mouse model, Exp. Dermatol. 27 (9) (2018) 1038–1042.
[66] Z. Wang, W. Yin, L. Zhu, J. Li, Y. Yao, F. Chen, M. Sun, J. Zhang, N. Shen, Y. Song, X. Chang, Iron drives T helper cell pathogenicity by promoting RNA-binding protein PCBP1-mediated proinflammatory cytokine production, Immunity 49 (1) (2018) 80–92 e7.